

Formation of fractal structure in many-body systems with attractive power-law potentials

Hiroko Koyama*

Department of Physics, Waseda University, Shinjuku, Tokyo, 169-8555, Japan

Tetsuro Konishi†

Department of Physics, Nagoya University, Nagoya, 464-8602, Japan

(Received 5 July 2005; published 18 January 2006)

We study the formation of fractal structure in one-dimensional many-body systems with attractive power-law potentials. Numerical analysis shows that the range of the index of the power for which fractal structure emerges is limited. Dependence of the growth rate on wave number and power-index is obtained by linear analysis of the collisionless Boltzmann equation, which supports the numerical results.

DOI: [10.1103/PhysRevE.73.016213](https://doi.org/10.1103/PhysRevE.73.016213)

PACS number(s): 05.45.Df, 05.65.+b

I. INTRODUCTION

Formation of spatial structures is an interesting and important phenomenon in nature. It is seen over a wide range, from protein folding in biological systems [1,2] to large-scale structure in the universe [3]. The theoretical origins of such structures are quite important and will be classified into several classes. One of the most interesting areas within the field of dynamical systems is that some remarkable structure and organization is created dynamically by the mutual interaction among the elements [4,5].

Recently, we have discovered that spatial structure with fractal distribution emerges spontaneously from uniformly random initial conditions in a one-dimensional self-gravitating system, that is the sheet model [6]. What is noteworthy in this phenomenon is that the spatial structure is not given at the initial condition, but dynamically created from a state without spatial correlation. Succeeding research clarified that the structure is created first in small spatial scale then grows up to large scale through hierarchical clustering [7], and the structure is transient [8]. It is quite interesting that some remarkable spatial structures are emerged instead of monotonous thermal relaxation in the Hamiltonian system.

The emergence of fractal structure is a typical example that systems of many degrees of freedom are self-organized by dynamics themselves. Hence, to clarify, its dynamical mechanism is very important subject toward understanding physics of self-organization of matter.

A way to clarify the dynamical mechanism is to know which class of pair potential can form the fractal structure. Here we note an important fact that fractal structure does not have characteristic spatial scale, nor does the potential of the sheet model, since the pair potential is power of the distance. Hence, the scale free property of potential may be a keystone to understand the dynamical mechanism. The question is if the fractal structure can be formed in not only the sheet model, but also other systems with power-law potentials.

In this paper, we study the possibility that the fractal structure can be formed in more general systems without characteristic spatial scale which is extended from sheet model. Here, we adopt the model as the system with attractive power-law potentials. At first we examine the formation of the fractal structure by numerical simulation for various values of the power index of the potential. Next, we perform linear analysis to consider the numerical results.

In Sec. II, we introduce many-body systems with power-law potentials. In Sec. III, we review the formation of power-law correlation in the sheet model. In Sec. IV, we carry out numerical simulation. In Sec. V, we analyze linear perturbation of the collisionless Boltzmann equation. The final section is devoted to summary and discussions.

II. MODEL

We consider the model where many particles with an uniform mass interact with purely attractive pair potential of power law, which is described by the Hamiltonian [9]

$$H = K + U = \sum_{i=1}^N \frac{p_i^2}{2} + \sum_{i=1}^{N-1} \sum_{j>i}^N |x_i - x_j|^\alpha, \quad (1)$$

where x_i and p_i are the position and momentum of a particle, respectively. The first term is kinetic energy and the second term is potential energy. For simplicity, in this paper, we consider the system where motion of particles is bounded to one-dimensional direction.

For the special case $\alpha=1$, the Hamiltonian (1) applies to a system of N infinite parallel mass sheets, where each sheet extends over a plane parallel to the yz plane and moves along the x axis under the mutual gravitational attraction of all the other sheets. The Hamiltonian of the sheet model [10–13] is usually written in the form

$$H = \sum_{i=1}^N \frac{p_i^2}{2} + \sum_{i=1}^{N-1} \sum_{j>i}^N |x_i - x_j|. \quad (2)$$

In the previous letters [6–8], we investigated the time evolution of the sheet model (2) to show that the fractal structure emerges from nonfractal initial conditions. In Secs.

*Email address: koyama@gravity.phys.waseda.ac.jp†Email address: tkonishi@r.phys.nagoya-u.ac.jp

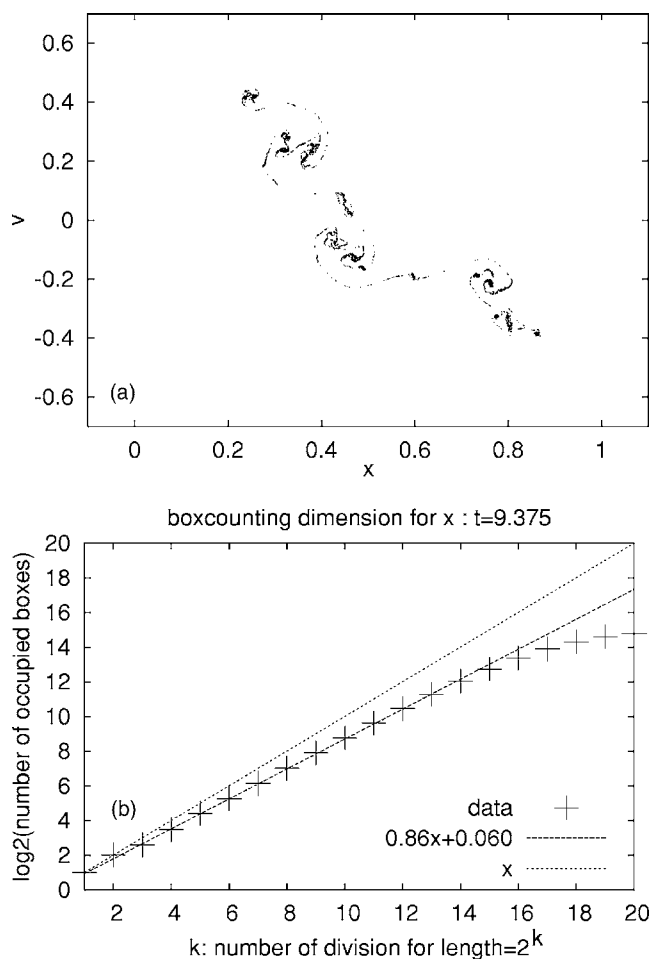


FIG. 1. An example of fractal structure is formed of the model (2) from a nonfractal structure. The number of particles is $N=2^{15}$. The left figure represents the μ space at $t=9.375$. The right figure represents the box counting dimension.

IV and V, we will clarify the relation between the power index of the pair potential α and the formation of the fractal structure by investigating time evolution of more general model (1) numerically and analytically.

III. FORMATION OF FRACTAL STRUCTURE IN THE SHEET MODEL ($\alpha=1$)

Before we investigate the time evolution of the model (1), we briefly review our previous works [6–8] on the model (2). We found that the fractal structure is formed in the sheet model (2) from uniformly random initial conditions [6,7]. In Fig. 1, we show a typical example of such a fractal structure and a snapshot of the μ -space configuration.

IV. NUMERICAL SIMULATION

In this section, we examine by computer simulations if the fractal structure is formed in the systems (1). Here we carry out the case $\alpha \geq 1$ to avoid divergence when two particles come close.

The nonfractal initial conditions where the fractal structure emerged are characterized typically by those of virial ratio $2E_{kin}/E_{pot}=0$ in the sheet model [6]. (Spatial distribution is set to be random.) This state of zero velocity dispersion corresponds to the limiting case of zero thermal fluctuation and is called the cold-random condition. Therefore, we adopt this cold-random initial condition to investigate the time evolution for various values of α . In our simulation we use the fourth order of the symplectic integrator with a fixed time step $\Delta t=2\pi/10^4$ and $N=65\,536$ particles. In what follows, we show numerical results for two typical examples: $\alpha=1.125$ and $\alpha=1.5$. For other values of α , behavior of the systems varies gradually in accordance with the change of α .

A. The case $\alpha=1.125$

At first, we consider the case when the interaction force deviates slightly from the sheet model. Here we show the numerical results in the case $\alpha=1.125$ in Figs. 2 and 3. We display particle distribution in (x, v) space (μ space) in Fig. 2. In the course of time evolution, we see that many whirlpools nest in the μ space to form the hierarchical structure. In Fig. 3, we show a box counting dimension of the spatial distribution. We can see that the dimension is $D \approx 0.83$ (Fig. 3). Therefore, our numerical results suggest that the fractal structure is formed. These behaviors are similar qualitatively to the sheet model, $\alpha=1$ [6]. We find that fractal structure can be formed as well as the sheet model.

B. The case $\alpha=1.5$

Next, we consider the interaction deviate further from the sheet model. Time evolution changes qualitatively as α increases. Here we show the numerical results in the case $\alpha=1.5$. We display particle distribution in μ space in Fig. 4, and in Fig. 5, we show a box counting dimension for spatial distribution. Differently from the case $\alpha=1.125$, a single spiral is rolled up in μ space. Therefore, fractal structure is not formed.

We can summarize these numerical results in this section: the fractal structure can be constructed as well as the sheet model, but the range of α , for which the fractal structure is created, is limited; it cannot be constructed for a large value of α .

V. ANALYSIS OF LINEAR PERTURBATION

In this section, we clarify the physical reason analytically why fractal structure cannot be constructed for the large value of the power index of the potential in numerical simulation in Sec. IV. The formation of the fractal structure occurs at the relative early stage in the whole-evolution history [8]. Then it is instructive for understanding the mechanism by which the structure is formed to know the qualitative properties of the short-term behaviors by linear analysis.

In this section, we derive the dispersion relation from the collisionless Boltzmann equation (CBE), which describes the growing rate of the linear perturbation [14,15].

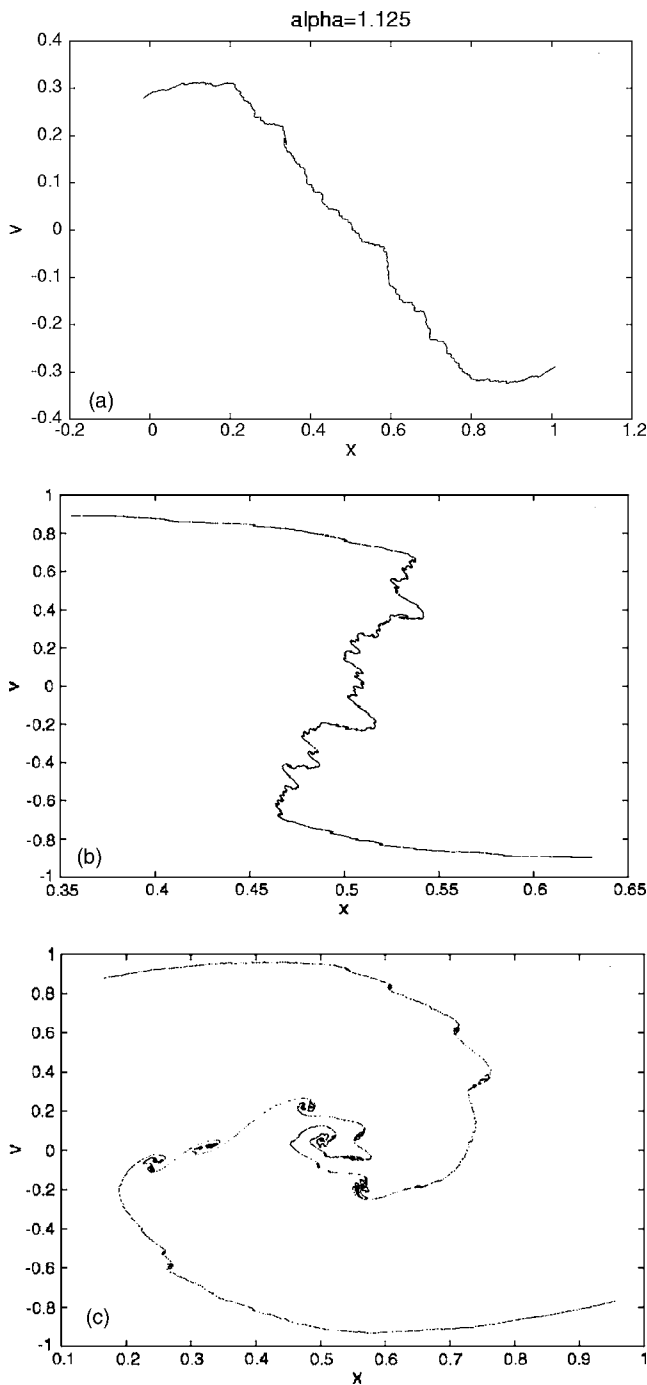


FIG. 2. The snapshots of the μ space for $\alpha=1.125$. $N=65\,536$. Times are $t=4.4, 5.0, 9.4$ from the top to the bottom.

A. Collisionless Boltzmann equation

CBE is defined by

$$\left\{ \frac{\partial}{\partial t} + p \frac{\partial}{\partial x} + \int_{-\infty}^{\infty} dx' F(x-x') \right. \\ \left. \times \left(\int_{-\infty}^{\infty} dp' f(x', p', t) \right) \frac{\partial}{\partial p} \right\} f(x, p, t) = 0, \quad (3)$$

where F is a two-particle force which is related with a pair-potential U by

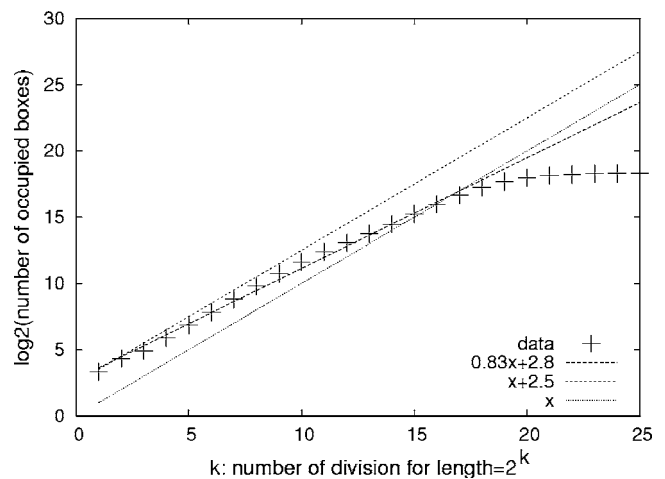


FIG. 3. Box counting dimension D of the spatial distribution for $\alpha=1.125$ and $t=5.0$. The plus symbols represent our data, and solid and dashed lines correspond to $D=0.83$ and $D=1$, respectively.

$$F(x) = - \frac{dU}{dx}, \quad (4)$$

and f is the one-particle distribution function. For simplicity, we consider that the system is extended in infinite region $-\infty < x < \infty$. It is clear that the state of uniform spatial density with an arbitrary velocity distribution,

$$f(x, p, t) = f_0(p), \quad (5)$$

is a stationary state. We impose the following small perturbation over the stationary state (5)

$$f(x, p, t) = f_0(p) + \delta f(x, p, t). \quad (6)$$

The linearized equation for δf is

$$\left(\frac{\partial}{\partial t} + p \frac{\partial}{\partial x} \right) \delta f(x, p, t) \\ = - \int_{-\infty}^{\infty} dx' F(x-x') \\ - x' \int_{-\infty}^{\infty} dp' \delta f(x', p', t) \frac{\partial}{\partial p} f_0(p). \quad (7)$$

Now we define the Fourier-Laplace transform by that x is Fourier transformed and t is Laplace transformed, that is

$$\widetilde{\delta f}(k, p, \omega) \equiv \int_0^{\infty} dt e^{-i\omega t} \int_{-\infty}^{\infty} dx e^{ikx} \delta f(x, p, t). \quad (8)$$

Fourier transform is

$$\hat{\delta f}(k, p, t) \equiv \int_{-\infty}^{\infty} dx e^{ikx} \delta f(x, p, t), \quad (9)$$

and

$$\hat{F}(k) \equiv \int_{-\infty}^{\infty} dx e^{ikx} F(x). \quad (10)$$

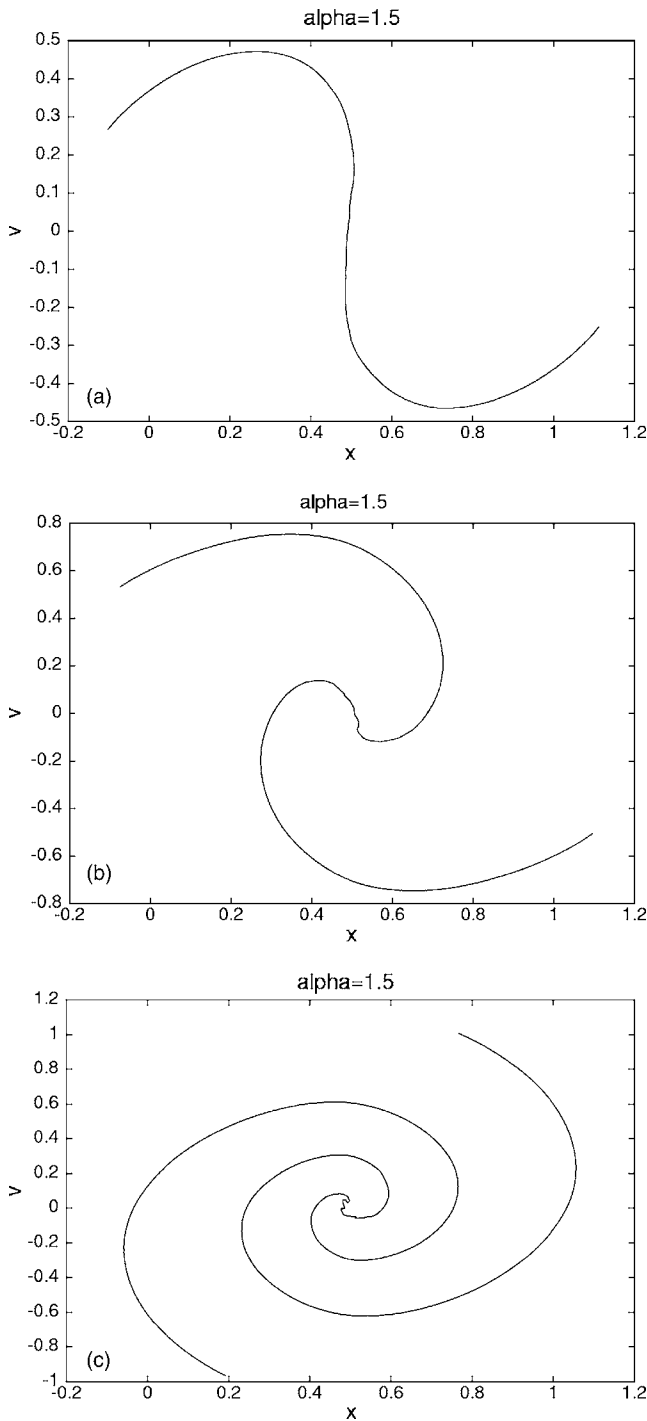


FIG. 4. The snapshots of the μ space for $\alpha=1.5$. $N=65\,536$. Times are $t=11.0$, 15.7 , and 23.6 from the top to the bottom.

Then the Fourier-Laplace transformed equation of Eq. (7) is

$$\varepsilon_k(\omega) \widetilde{\delta f_k}(\omega) = \frac{-1}{i(-\omega + kp)} \hat{\delta f}(k, p, 0), \quad (11)$$

where $\varepsilon_k(\omega)$ is

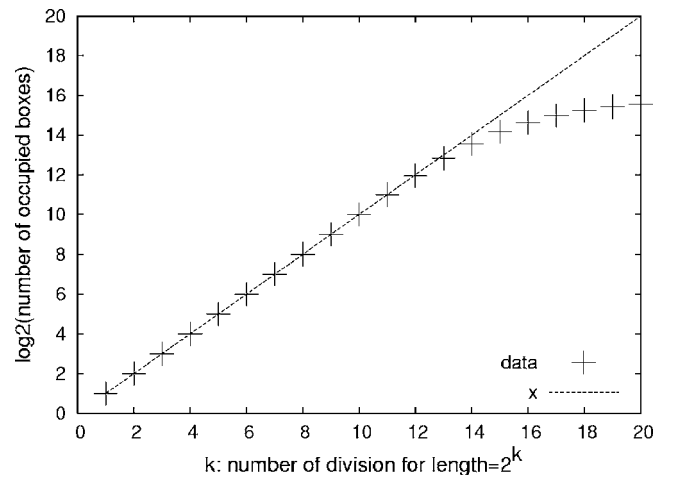


FIG. 5. Box counting dimension D of the spatial distribution for $\alpha=1.5$ and $t=23.6$.

$$\varepsilon_k(\omega) \equiv 1 + \int_{-\infty}^{\infty} dp \frac{\hat{F}(k)}{i(-\omega + kp)} \frac{\partial f_0}{\partial p}(p). \quad (12)$$

B. Dispersion relation

From the inverse-Laplace transform of Eq. (11),

$$\delta f_k(t) = \int_{-\infty-i\sigma}^{\infty-i\sigma} e^{i\omega t} \widetilde{\delta f_k}(\omega) \frac{d\omega}{2\pi} \quad (13)$$

$$= \int_{-\infty-i\sigma}^{\infty-i\sigma} e^{i\omega t} \frac{1}{\varepsilon_k(\omega)} \frac{-1}{i(-\omega + kp)} \hat{\delta f}(k, p, 0) \frac{d\omega}{2\pi}. \quad (14)$$

Now we continuously move the integration contour to the upper half of complex ω plane while avoiding the singular points. Then the contributions from except of the pole can be neglected, because of the factor $\exp(i\omega t)$ [$\text{Im}(\omega) > 0$].

Then the growth rate of each mode of the fluctuation is obtained by the solution of the equation

$$\varepsilon_k(\omega) = 0. \quad (15)$$

Equation (15) is the dispersion relation. If Eq. (15) has the solution where the inequality $\text{Im}(\omega) < 0$ is satisfied, the fluctuation is unstable.

C. Dynamical stability of systems with power-law potentials

Now we consider the case that the potential is power law, the pair-potential U is

$$U(x) = A|x|^\alpha. \quad (16)$$

Assuming the interaction is attractive, $A > 0$. $\alpha=1$ for the “sheet model.” The Fourier-transformed potential is [16]

$$\hat{U}(k) \equiv \int_{-\infty}^{\infty} dx e^{ikx} A|x|^\alpha \quad (17)$$

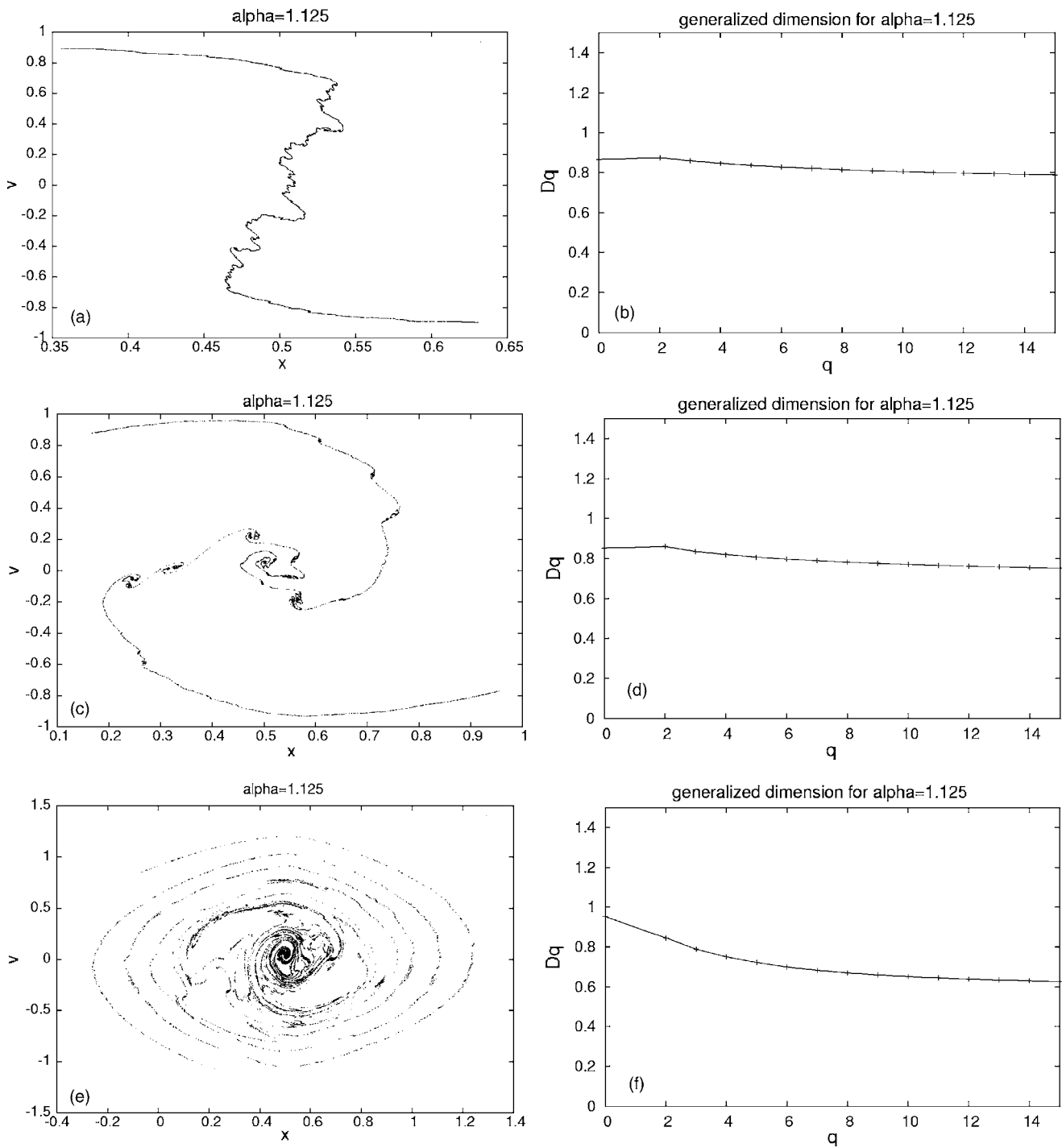


FIG. 6. The snapshot of the μ space for $\alpha=1.125$ (left). The generalized dimension D_q (right). Times are $t=5.0, 9.4,$ and 37.7 from the top to the bottom.

$$=2A \left\{ - \left(\sin \frac{\alpha\pi}{2} \right) \frac{\Gamma(\alpha+1)}{|k|^{\alpha+1}} \right\} \quad (\alpha \neq 0, 2, 4, \dots, -1, -3, \dots). \tag{18}$$

For simplicity, we choose the stationary state as

$$f_0 = n_0 \delta(p), \tag{19}$$

where n_0 is the number density of particles.

The dispersion relation is

$$\epsilon_k(\omega) = 1 + 2n_0 A \left\{ \left(\sin \frac{\alpha\pi}{2} \right) \frac{\Gamma(\alpha+1)}{|k|^{\alpha-1}} \right\} \frac{1}{\omega^2} = 0, \tag{20}$$

and ω , which satisfies the dispersion relation is

$$\omega^2 = -2n_0A \left\{ \left(\sin \frac{\alpha\pi}{2} \right) \frac{\Gamma(\alpha+1)}{|k|^{\alpha-1}} \right\}. \quad (21)$$

When $\omega^2 < 0$, the system is unstable. Equation (21) can be reduced to

$$\omega = \pm i \sqrt{2n_0A \left\{ \left(\sin \frac{\alpha\pi}{2} \right) \Gamma(\alpha+1) \right\} |k|^{(1-\alpha)/2}}. \quad (22)$$

From Eq. (22), we can classify the evolution of the perturbation into three types: (i) when $0 < \alpha < 1$, the growing rate increases monotonously for $|k|$; (ii) when $\alpha = 1$, the fluctuations for the entire scale grows at same rate; (iii) when $1 < \alpha < 2$, the growing rate decreases monotonously for $|k|$.

The cold-random condition corresponds to the mixed states of fluctuation with all wavelengths, the so-called “white noise.” The larger the value of α is, the smaller the growth rate of the fluctuation with a large wave vector is. This is consistent with the numerical results in Sec. IV that a large whirlpool is formed in μ space in the case for the large value of α .

VI. CONCLUDING REMARK

In this paper, we have studied structure formation of many-body systems with power-law potentials. First, we have investigated structure formation in this model by numerical simulation. As a result, we have found that behaviors of time evolution are different depending on the power index of the potential. When α is slightly above 1, the fractal structure is formed similar to the sheet model [6]. On the other hand, when $\alpha \geq 1.5$, the fractal structure is not formed.

In order to explain these numerical results, we have also analyzed linear perturbation of the collisionless Boltzmann equation to derive the dispersion relation, which represents the growth rate of each mode of the fluctuation. As a result, we have found that for a large value of α , the growth rate of the small scale is suppressed. In addition, we can explain the sheet model ($\alpha = 1$) is marginal in the sense that all scale fluctuations grow at the same rate. There is a slight difference between the initial condition used in the numerical simulation and the stationary state employed in the perturbation, that is, we set N particles in a finite region for simulation, whereas the unperturbed state f_0 is infinitely spread. Nonetheless, we think the linear perturbation grabs the core of the instability, especially for a short time scale.

In our simulation, the fractal structure is formed through hierarchical clustering. That is, clusters are created first in a small spatial scale, then grow to a large scale [7]. The spatial randomness in the initial condition and finiteness of the number of particles N imply that relative fluctuation in mass density is large for the small spatial scale. This enhancement of initial fluctuation in a small spatial scale is probably the “seed” of spatial structure formation.

Fractal properties of the structures can differ from place to place of the system. Most fractal structures are not exactly self-similar but can contain various inner structures. Using generalized dimension D_q [17], one can unveil details of fractal structures. Here we show the generalized dimension

of the spatial structure formed in the power-law potential model with $\alpha = 1.125$ in Fig. 6. We find that the generalized dimension is almost constant ($D_q \approx 0.83$) for some range of q at $t = 5.0$ (Fig. 6, top). Therefore, we conclude that the fractal structure formed is *monofractal* at $t = 5.0$, as far as we observed.

As discussed in our previous paper [8], however, the fractal structure is a transient state and relaxes finally. We find that the multifractal nature emerges due to the relaxation at late times (the bottom of Fig. 6). The box counting dimension D_0 has relaxed to almost 1, while the correlation dimension D_2 has not yet (the bottom of Fig. 6). In other words, the relaxation of the box counting dimension D_0 is much faster than the correlation dimension D_2 . The detailed analysis will be a future work.

We noted that the scale-free property of the potential may be a keystone to understand the dynamical mechanism of the emergence of fractal spatial structure. In this paper, we have clarified that scale-free property does not immediately imply fractal structure. Potentials with different power indices make different temporal behaviors, and the gravitational system (the sheet model) is a special case in all the one-dimensional systems with scale-free potential.

Structure formation in other one-dimensional self-gravitating systems in an expanding universe has been studied in relevant works [13,18]. They claimed that their system is not a simple fractal or even a regular multifractal, but bifractal [13]. Indications of this behavior have also been found for the “quintic” model [19]. It is a future work to clarify the relevance between the models comprehensibly. In addition, the dependence of the spatial dimension on the structure formation will be an interesting and important subject of future works.

ACKNOWLEDGMENTS

We would like to thank Angelo Vulpiani for useful comments. H. K. is supported by JSPS Foundation for Young Scientists. T. K. is supported by Grant-in-Aid for Scientific Research from the Ministry of Education, Culture, Sports, Science, and Technology of Japan.

APPENDIX: PROOF OF EQ. (11)

In this appendix, we lead Eq. (11) by the Fourier-Laplace transform of Eq. (7). In terms of the transform (11), Eq. (7) become following: The first term of the left-hand side of Eq. (7) is transformed to

$$\begin{aligned} & \int_0^\infty dt e^{-i\omega t} \int_{-\infty}^\infty dx e^{ikx} \frac{\partial}{\partial t} \delta f(x, p, t) \\ &= [e^{-i\omega t} \hat{\delta} f(k, p, t)]_{t=0}^{t=\infty} - (-i\omega) \int_0^\infty dt e^{-i\omega t} \hat{\delta} f(k, p, t) \end{aligned} \quad (A1)$$

$$= -\hat{\delta} f(k, p, t=0) + i\omega \widetilde{\delta f}(k, p, \omega), \quad (A2)$$

here ω is a complex number and $\text{Im } \omega < 0$. The second term of the left-hand side of Eq. (7) is transformed to

$$\int_0^\infty dt e^{-i\omega t} \int_{-\infty}^\infty dx e^{ikx} p \frac{\partial}{\partial x} \delta f(x, p, t) = -ikp \int_0^\infty dt e^{-i\omega t} \hat{\delta} f(k, p, t) \\ = -ikp \widetilde{\delta f}(k, p, \omega). \quad (\text{A3})$$

Then the left-hand side of Eq. (7) is transformed to

$$(lhs) = -i(-\omega + kp) \widetilde{\delta f}(k, p, \omega) - \widetilde{\delta f}(k, p, 0). \quad (\text{A4})$$

On the other hand, the right-hand side of Eq. (7) is transformed to

$$(rhs) = - \int_0^\infty dt e^{-i\omega t} \int_{-\infty}^\infty dx e^{ikx} \left\{ \int_{-\infty}^\infty dx' F(x - x') \right. \\ \left. \times \int_{-\infty}^\infty dp' \delta f(x', p', t) \frac{\partial}{\partial p} f_0(p) \right\} \\ = \int_{-\infty}^\infty dy e^{iky} F(y) \int_{-\infty}^\infty dp' \widetilde{\delta f}(k, p', \omega) \frac{\partial f_0}{\partial p}(p) \\ = \hat{F}(k) \int_{-\infty}^\infty dp' \widetilde{\delta f}(k, p', \omega) \frac{\partial f_0}{\partial p}(p),$$

where

$$\widetilde{\delta f}(x', p', \omega) \equiv \int_0^\infty dt e^{-i\omega t} \delta f(x', p', t). \quad (\text{A5})$$

Equation (7) is transformed to

$$\widetilde{\delta f}(k, p, \omega) = \left(\frac{-\hat{F}(k)}{i(-\omega + kp)} \frac{\partial f_0}{\partial p}(p) \right) \left(\int_{-\infty}^\infty dp' \widetilde{\delta f}(k, p', \omega) \right) \\ + \frac{-1}{i(-\omega + kp)} \hat{\delta} f(k, p, 0), \quad (\text{A6})$$

where

$$\widetilde{\delta f}_k(\omega) \equiv \int_{-\infty}^\infty dp \widetilde{\delta f}(k, p, \omega).$$

Integrating both sides of Eq. (A6) by p , we obtain

$$\left(1 + \int_{-\infty}^\infty dp \frac{\hat{F}(k)}{i(-\omega + kp)} \frac{\partial f_0}{\partial p}(p) \right) \widetilde{\delta f}_k(\omega) \\ = \frac{-1}{i(-\omega + kp)} \hat{\delta} f(k, p, 0). \quad (\text{A7})$$

Using Eq. (12), we obtain Eq. (11).

-
- [1] A. Fersht, *Structure and Mechanism in Protein Science* (W. H. Freeman, New York, 1998).
- [2] M. Karplus, *J. Phys. Chem. B* **104**, 11 (2000).
- [3] P. J. E. Peebles, *The Large Scale Structure of the Universe* (Princeton University Press, Princeton, NJ, 1980).
- [4] T. Dauxois, P. Holdsworth, and S. Ruffo, *Eur. Phys. J. B* **16**, 659 (2000).
- [5] J. Barré, T. Dauxois, and S. Ruffo, *Physica A* **295**, 254 (2001).
- [6] H. Koyama and T. Konishi, *Phys. Lett. A* **279**, 226 (2001).
- [7] H. Koyama and T. Konishi, *Europhys. Lett.* **58**, 356 (2002).
- [8] H. Koyama and T. Konishi, *Phys. Lett. A* **295**, 109 (2002).
- [9] Lj. Milanović, H. A. Posch, and W. Thirring, *Phys. Rev. E* **57**, 2763 (1998).
- [10] F. Hohl and M. R. Feix, *Astrophys. J.* **147**, 1164 (1967).
- [11] G. B. Rybicki, *Astrophys. Space Sci.* **14**, 56 (1971).
- [12] M. Luwel, G. Severne, and P. J. Rousseeuw, *Astrophys. Space Sci.* **100**, 261 (1984).
- [13] B. N. Miller and C. J. Reidl, Jr., *Astrophys. J.* **348**, 203 (1990).
- [14] J. Binney and S. Tremaine, *Galactic Dynamics* (Princeton University Press, Princeton, NJ, 1987).
- [15] S. Inagaki and T. Konishi, *Publ. Astron. Soc. Jpn.* **45**, 733 (1993).
- [16] M. J. Lighthill, *An Introduction to Fourier Analysis and Generalised Functions* (Cambridge University Press, Cambridge, 1958).
- [17] T. C. Halsey, M. H. Jensen, L. P. Kadanoff, I. Procaccia, and B. I. Shraiman, *Phys. Rev. A* **33**, 1141 (1986).
- [18] J-L. Rouet, M. R. Feix, and M. Navet, *Fractals in Astronomy*, A. Heck, *Vistas Astron.* **33**, 357 (1990).
- [19] E. Aurell, D. Fanelli, and P. Muratore-Ginanneschi, *Physica D* **148**, 272 (2001).